



Reliability Analysis of Blade Fatigue Life Based on Fuzzy Intelligent Multiple Extremum Response Surface Method

Chun-Yi Zhang^a, Tian Sun^a, Ai-Hua Wang^a, Hui-Zhe Jing^a, Bao-Sheng Liu^a, Cheng-Wei Li^a

^aSchool of Mechanical and Power Engineering, Harbin University of Science and Technology, Harbin 150080, China

Abstract. In order to more reasonable analyze the dynamic reliability of aero-engine blade with coupling failure mode. A fuzzy intelligent multiple extremum response surface method (FIMERSM) was proposed. Considering the coupling effect of temperature load and centrifugal load, the maximum stress point, the maximum strain point and the minimum life point on blade were found by deterministic analysis. Then, the density of blade, rotor speed, elastic modulus, blade-tip temperature, blade-root temperature, fatigue strength coefficient, fatigue strength exponent, fatigue ductility coefficient, fatigue ductility exponent, blade width, blade thickness, blade torsion angle, and blade height as input random variables. By using Latin hypercube sampling technique, the sample values of the input random variables were acquired and finite element basic equation was calculated for each samples which obtained the corresponding dynamic output response of their stress, strain, and low cycle fatigue life within the analysis time domain. By taking the entire maximum values of the dynamic output response in the analysis time domain as new output response, the fuzzy intelligent multiple extremum response surface function (FIMERSF) was established. Finally, the dynamic reliability of the blade structure were obtained by using the Monte Carlo method (MCM) large amount linkage sampling of the input random variables and take it into the FIMERSF to calculate the output response. The results imply that the comprehensive reliability of blade is 99.46%. Through the comparison of MCM, Multiple extremum response surface method (MERSM) and FIMERSM, the computational results show that the FIMERSM has high computational precision and computational efficiency.

Introduction

Turbine blade, as an important component of aero-engine, bears complex failure modes such as stress, strain and low-cycle fatigue, and subjected to heavy loads such as high temperature, high pressure and high revolving speed. Therefore, it is important to analyze the reliability of turbine blade [1].

The classical reliability analysis method has been studied extensively [2-4]. Among them, the Response surface method (RSM) is fast and certain precision, and it widely used in the field of reliability analysis. Hu-Yun et al. [5] calculated the reliability of gear by RSM with consideration the effects of elasto hydrodynamic lubrication (EHL) on contact fatigue reliability of gear. Some scholars have improved the response surface

2010 *Mathematics Subject Classification.* 03B52.

Keywords. Fuzzy; Intelligent multi-extremum response surface; Monte carlo; Dynamic reliability; Thermo-structural coupling.

Received: 20 September 2017; Accepted: 20 November 2017

Communicated by Hari M. Srivastava

Corresponding Author: Chun-Yi Zhang, Tel.:+86 18846082897

This study is supported by the National Natural Science Foundation of China (Grant No. 51275138) and the project of Chinese Heilongjiang Province Education Department (Grant No. 12531109)

Email address: zhangchunyi666@sina.com. (Chun-Yi Zhang)

method to improve its computational speed and computational accuracy. Zhang Chun-yi et al. [6] firstly proposed the thought of the extremum response surface method (ERSM), and completed the reliability analysis of the two-link flexible manipulator by using extremum response surface function instead of the dynamic differential equation of the Lagrange form of the flexible mechanism. Gao Hai-Feng et al. [7] established the Manson-Coffin formulas of nickel-based superalloy GH4133 of aeroengine blade material based on the different confidence levels, and completed the prediction of the low-cycle fatigue life (LCF) of turbine blade with thermo-structural coupling interaction by distributed collaborative response surface method (DCRSM). However, due to the fact that scientific research has its own development law, the reliability analysis were carried out in one failure mode at that time, without considering the correlation between the failure modes, and the fuzzy properties of the constraint boundary conditions.

The support Vector Regression (SVR) is a kind of machine intelligence algorithm [8], which has an excellent learning ability of small sample and efficient computational efficiency, and it widely used in the field of reliability analysis [9-11]. In the traditional SVR, it is necessary to give the value of the insensitive parameter ε in advance, and it is difficult to select the reasonable value of ε in the practical application. Then, Schölkopf et al. [12] proposed V-Support Vector Regression (V-SVR), introduced the ε -loss function control parameter ν in the original optimization problem of SVR, and solved ε as constraint of optimization problem. However, V-SVR is susceptible to the influence of noise and outliers when there is a lot of fuzzy information in the training samples. Therefore, Yan Hong-Sen et al. [13] proposed a Fuzzy V-Support Vector Regression (FV-SVR) by combining the fuzzy regression theory with the V-SVR, and applied it to the product design time intelligent estimation. However, FV-SVR has not been applied to reliability analysis.

In order to improve the calculation accuracy and calculation efficiency of reliability analysis, considering the correlation between failure modes, and the fuzziness of data. A method of FIMERSM was proposed by integrating FV-SVR and RSM, and applied it to the dynamic reliability analysis of aeroengine turbine blades and comparison with other reliability analysis methods shows that FIMERSM has strong advantages.

1. Fuzzy Intelligent Multi-Extremum Response Surface Method

1.1. Basic thought

The basic principle of FIMERSM is as follows: the material performance parameters, working conditions and design dimensions of the blade were selected as input variables. Considering the coupling effect of temperature load and centrifugal load, the basic equations of the finite element of the blade are solved, and the maximum stress point, the maximum strain point and the minimum life point of the blade are found by deterministic analysis. Then, considering the randomness and fuzziness of the data, the above input variable is taken as the input random variable, and the sample of the random variable is extracted by using the Latin hypercube sampling technique. The dynamic output response of the stress, strain, and low cycle fatigue life with in the analysis time domain were obtained by solve the finite element basic equation for each samples. By taking the entire maximum values of the dynamic output response in the analysis time as the new output responses, and the data is normalized as the training sample of the FV-SVR model. The parameters of FV-SVR is optimized by genetic algorithm (GA), the fuzzy intelligent multiple extremum response surface function (FIMERSF) was established. Finally, the dynamic reliability of the blade structure were obtained by using MCM large amount linkage sampling of the input random variables and bring them into the FIMERSF to calculate the output responses.

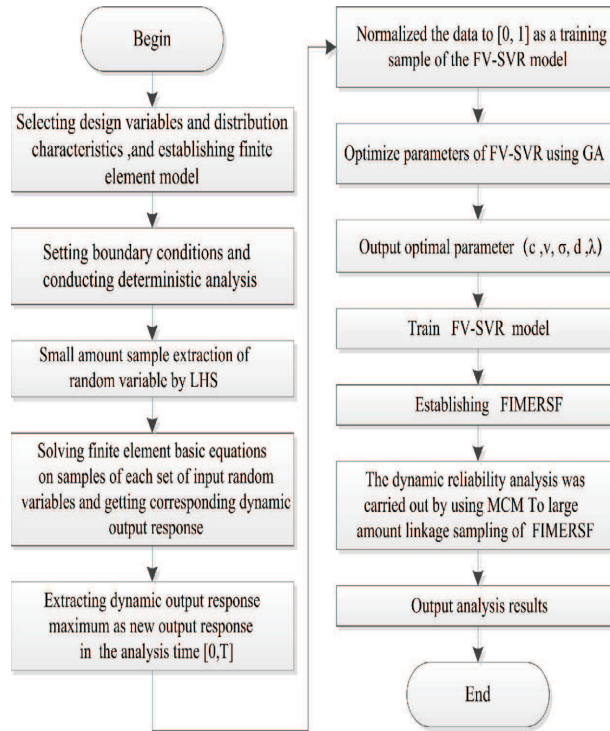


Figure 1 The FEM of blade

1.2. Mathematical model

1.2.1. Mathematical model of FV-SVR

Given a training dataset $\{(x_i, y_i), x_i \in T(R)^n, y_i \in T(R), i = 1, 2, \dots, l\}$, $x_i \in T(R)^n$ is an input sample, $y_i \in T(R)$ is the output value. $T(R)$ and $T(R)^n$ is the space of 1-dimensional and n-dimensional of triangular fuzzy numbers, respectively. In order to simplify the calculation, the symmetric triangular fuzzy numbers are taken into account, i.e. $s_{x_i} = t_{x_i}, s_{y_i} = t_{y_i}, x_i = (m_{x_i}, s_{x_i}), y_i = (m_{y_i}, s_{y_i})$. m, s and t represent the central, left and right fuzzy amplitudes of the triangular fuzzy numbers, respectively. The FV-SVR is modeled by minimizing following constrained risk function [13] in Eq. (1).

$$\min_{w, b, \varepsilon, \xi^{(k)}} \frac{1}{2} \|w\|^2 + c[v\varepsilon + \frac{1}{l} \sum_{k=1}^2 \sum_{i=1}^l (\xi_{ki} + \xi_{ki}^*)] \tag{1}$$

$$s.t \begin{cases} (m_{y_i} + s_{y_i}) - w \cdot \Phi(m_{x_i}) - b - \rho(s_{x_i}) \leq \varepsilon + \xi_{1i} \\ w \cdot \Phi(m_{x_i}) + b + \rho(s_{x_i}) - (m_{y_i} + s_{y_i}) \leq \varepsilon + \xi_{1i}^* \\ (m_{y_i} - s_{y_i}) - w \cdot \Phi(m_{x_i}) + b - \rho(s_{x_i}) \leq \varepsilon + \xi_{2i} \\ w \cdot \Phi(m_{x_i}) + b - \rho(s_{x_i}) - (m_{y_i} - s_{y_i}) \leq \varepsilon + \xi_{2i}^* \\ \xi_{ki}, \xi_{ki}^* \geq 0, k = 1, 2 \\ \varepsilon \geq 0 \end{cases} \tag{2}$$

Where, $\|w\|^2 = \sum_{i,j=1}^l (a_{1i} - a_{1i}^* + a_{2i} - a_{2i}^*)(a_{1j} - a_{1j}^* + a_{2j} - a_{2j}^*)(\Phi(m_{x_i}) \cdot \Phi(m_{x_j}))$; $\rho(s_{x_i}) = \max\{s_{x_{i1}}, \dots, s_{x_{in}}\}$ is maximum fuzzy amplitude of x_i ; $\Phi(\cdot)$ denotes a nonlinear mapping function from the input space x_i to a high-dimensional feature space; c is the regularization constant; $v \in [0, 1]$ is a control parameter of ε -loss function; $\xi_{ki}, \xi_{ki}^* (k = 1, 2; i = 1, \dots, l)$ are the slack variables; w and b are the support vector weight and the bias. By introducing the Lagrange multiplier a_{ki}^* , the mathematical model of FV-SVR is obtained by solving

the above optimization problem.

$$\tilde{y} = f(x) = \left(\sum_{k=1}^2 \sum_{i=1}^l (a_{ki} - a_{ki}^*) K(\mathbf{m}_{x_i}, \mathbf{m}_{x_j}) + b, \rho(s_x) \right) \quad (3)$$

In the formula (3), $k(\mathbf{m}_{x_i}, \mathbf{m}_{x_j})$ is the kernel function, the Gaussian radial basis kernel function $k_{RBF}(\mathbf{m}_{x_i}, \mathbf{m}_{x_j})$ and the polynomial kernel function $k_{poly}(\mathbf{m}_{x_i}, \mathbf{m}_{x_j})$ are combined to construct the mixed kernel function as follows [14]:

$$K_{mix}(\mathbf{m}_{x_i}, \mathbf{m}_{x_j}) = \lambda[(\mathbf{m}_{x_i} \cdot \mathbf{m}_{x_j}) + 1]^d + (1 - \lambda) \exp \left\{ -\frac{\|\mathbf{m}_{x_i} - \mathbf{m}_{x_j}\|^2}{2\sigma^2} \right\} \quad (4)$$

Where, $0 < \lambda < 1$ is the mixed kernel function weighting factor; σ, d is the kernel function parameter of RBF kernel and polynomial kernel, respectively.

1.2.2. Mathematical model of FIMERSM

The basic thought of FIMERSM is as follows: $X^{(j)}$ is assumed to be the input vector sample values of member group j . The maximum value of the responses at time domain $[0, T]$ is $y_{\max}^{(j)}(X^{(j)})$. The set of $y_{\max}^{(j)}(X^{(j)})$ is $\{y_{\max}^{(j)}(X^{(j)}) : j \in Z_+\}$. The relationship of $X^{(j)}$ and y can be expressed in the following function:

$$y = f(X) = \{y_{\max}^{(j)}(X^{(j)}) : j \in Z_+\} \quad (5)$$

Where, Z_+ is positive integer. Through the establishment of multiple extremum response surface function (MERSF) [6] by FV-SVR for each failure mode, the mathematical model of fuzzy intelligent multiple extremum response surface method is shown as follows:

$$\begin{cases} \tilde{y}_{\max}^{(1)} = f(X^{(1)}) = \left(\sum_{k=1}^2 \sum_{i=1}^l (a_{ki} - a_{ki}^*)^{(1)} k_{mix}(\mathbf{m}_{x_i}, \mathbf{m}_{x_j})^{(1)} + b^{(1)}, \rho(s_x)^{(1)} \right) \\ \tilde{y}_{\max}^{(2)} = f(X^{(2)}) = \left(\sum_{k=1}^2 \sum_{i=1}^l (a_{ki} - a_{ki}^*)^{(2)} k_{mix}(\mathbf{m}_{x_i}, \mathbf{m}_{x_j})^{(2)} + b^{(2)}, \rho(s_x)^{(2)} \right) \\ \vdots \\ \tilde{y}_{\max}^{(j)} = f(X^{(j)}) = \left(\sum_{k=1}^2 \sum_{i=1}^l (a_{ki} - a_{ki}^*)^{(j)} k_{mix}(\mathbf{m}_{x_i}, \mathbf{m}_{x_j})^{(j)} + b^{(j)}, \rho(s_x)^{(j)} \right) \end{cases} \quad (6)$$

Where, $\tilde{y}_{\max}^{(j)}$ is the extremum output response with the j th failure modes; $(a_{ki} - a_{ki}^*)^{(j)}$ is the Lagrange multipliers with the j th failure modes; $k_{mix}(\mathbf{m}_{x_i}, \mathbf{m}_{x_j})^{(j)}$ is the mixed kernel function with the j th failure modes; $b^{(j)}$ is a bias term with the j th failure modes; $\rho(s_x)^{(j)}$ is the maximum fuzzy amplitude with the j th failure modes.

1.2.3. Mathematical model of Fuzzy reliability analysis

Assuming that the stress $S = S(x_1, x_2, \dots, x_n)$ and the intensity $R = R(x_1, x_2, \dots, x_n)$ of the structure are independent of each other, the structure is safe when $R > S$, and the structure is failure when $R < S$. By the transformation of the normalization factor F , we can establish a unified reliability model with both randomness and fuzziness, and F is defined as follows:

$$F = \iint u_R(r) f_R(r) u_S(s) f_S(s) u_{\xi}(m) dx_1 dx_2 \dots dx_n \quad (7)$$

Where, $f_S(s)$ and $f_R(r)$ represent the probability density functions of S and R , respectively. $u_S(s), u_R(r)$ represent the fuzzy membership functions of S and R , respectively. The membership function of the state

variable $M = R - S$ belongs to the security domain \tilde{S} is $u_{\tilde{S}}(m)$. By the conversion of the equivalent probability density function of the membership function of fuzzy variables, the problem of the generalized fuzzy stochastic reliability probability can be solved by the method of the stochastic reliability probability. The membership is transformed as follows:

$$u_i^{(e)}(x_i) = \frac{u_i(x_i)}{\int u_i(x_i) dx_i}, i = 1, 2, \dots, n_f \tag{8}$$

Based on the above-defined normalization factor F and the equivalent transformation probability density function $u_i(x_i) = u_i^{(e)}(x_i) \int u_i(x_i) dx_i$ of the fuzzy membership function, the fuzzy stochastic reliability probability p_r and failure probability p_f are defined as the integral form [15]:

$$p_r = \frac{\prod_{i=1}^{n_f} \int u_i(x_i) dx_i}{F} \iint_{R>S} u_R(r) f_R(r) u_S(s) f_S(s) u_{\tilde{S}}(m) dx_1 dx_2 \dots dx_n \tag{9}$$

$$p_f = 1 - p_r \tag{10}$$

2. Example

2.1. Thermal- structural coupling deterministic analysis of blade

An aeroengine turbine blade was selected as the example in the study and its material is GH4133B alloy [16]. The material performance parameters, working conditions and design dimensions [7] of the blade were selected as input random variables obeying normal distributions with mutual independence. The distributions of input random variables are shown in Table 1.

The blade was divided into 97795 tetrahedrons units and 160516 nodes. The finite element model (FEM) of blade are shown in Figure 1. The finite element basic equations (shape function of tetrahedron [17], geometric equation [18], physical equation [19], Manson-coffin formula [7] and Miner linear accumulative damage law [20]) of the thermal- structural coupling deterministic analysis of blade are shown in Eq. (11)-Eq. (15). The thermal-structure coupling deterministic analysis was completed by substituting the mean values in Table 1 into the finite element basic equations of the blade structure. The distributions of stress, strain and low-cycle fatigue life of blade are shown in Figure 2, Figure 3 and Figure 4. As can be seen from the analysis results, the maximum stress, maximum strain and minimum fatigue life of blade are locates on the blade-root.

Table 1 Input random variables of blade reliability analysis

Random variables	Mean	Standard deviation	Distribution
Density, $\rho / (\text{kg} \cdot \text{m}^{-3})$	8210	410.5	Normal
Rotor speed, $\omega / (\text{rad} \cdot \text{s}^{-1})$	1168	58.4	Normal
Elastic modulus, E / MPa	163000	4890	Normal
Blade -tip temperature, T_a / k	1473.15	73.658	Normal
Blade-root temperature, T_b / k	1173.2	60.658	Normal
Fatigue strength coefficient, σ_f	1419	70.95	Normal
Fatigue strength exponent, b	-0.1	0.005	Normal
Fatigue ductility coefficient, ϵ_{rf}	50.5	2.525	Normal
Fatigue ductility exponent, c	-0.84	0.042	Normal
Blade width, w / mm	41.1602	1.234806	Normal
Blade thickness, t / mm	8.1968	0.245904	Normal
Blade torsion angle, δ / radian	0.5458	0.016374	Normal
Blade height, h / mm	103.8536	3.115608	Normal

$$N_i = \frac{1}{6v}(a_i + b_i x + c_i y + d_i z)(i = 1, 2, 3, 4) \tag{11}$$

$$\begin{cases} \varepsilon_x = \frac{\partial u}{\partial x}, \varepsilon_y = \frac{\partial v}{\partial y}, \varepsilon_z = \frac{\partial w}{\partial z} \\ \gamma_{xy} = \frac{\partial u}{\partial y} + \frac{\partial v}{\partial x}, \gamma_{yz} = \frac{\partial v}{\partial z} + \frac{\partial w}{\partial y}, \gamma_{zx} = \frac{\partial w}{\partial x} + \frac{\partial u}{\partial z} \end{cases} \tag{12}$$

$$\{\sigma\} = [D] \{\varepsilon\} \tag{13}$$

$$\frac{\Delta\varepsilon}{2} = \frac{\sigma' f - \sigma_m}{E} (2N_f)^b + \varepsilon' f (2N_f)^c \tag{14}$$

$$D = \sum_{i=1}^r \frac{n_i}{N_i} \tag{15}$$

Where, v is the volume of tetrahedron; a_i, b_i, c_i, d_i is the related coefficient of node geometry; $\varepsilon_x, \varepsilon_y, \varepsilon_z$ and $\gamma_{xy}, \gamma_{yz}, \gamma_{zx}$ are the elastic body line strain and shear strain along the x, y, z direction, respectively; $\{\sigma\} = [\sigma_x, \sigma_y, \sigma_z, \tau_{xy}, \tau_{yz}, \tau_{zx}]$ is the components of stress; $[D]$ is the elastic matrix; $\{\varepsilon\} = [\varepsilon_x, \varepsilon_y, \varepsilon_z, \gamma_{xy}, \gamma_{yz}, \gamma_{zx}]$ is the components of strain; σ_m is the mean stress; $\Delta\varepsilon/2$ is the strain amplitude; D denotes damage; r is the number of stress levels; n_i is the cycle number of the i th level; N_i is the corresponding fatigue life of the i th stress levels.



Figure 2 The FEM of blade

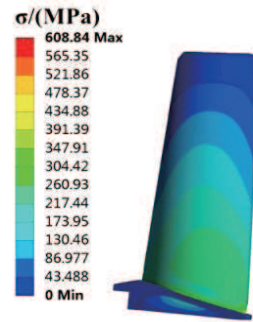


Figure 3 Distribution of blade stress

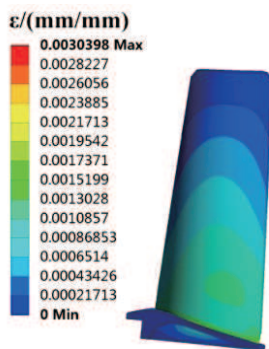


Figure 4 Distribution of blade strain

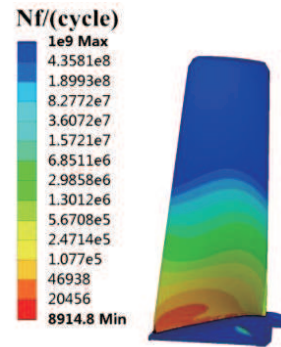


Figure 5 Distribution of blade life

2.2. Establishment Model of FIMERSM

The input random variables were sampled by the LHS [21] at the location of maximum stress, strain and minimum life of the blade. The output response values were obtained by thermal- structural coupling analysis based on these samples. The data is normalized to [0, 1] as a training sample for FV-SVR. In order to improve the prediction accuracy of FV-SVR model, the parameters of FV-SVR model (c, v, σ, λ, d) in

formula (1) and formula (4) are optimized by genetic algorithm (GA). The fitness function of GA is defined as the root mean square error (RMSE) of the k-fold cross validation method on the training data set, as follows [22]:

$$RMSE = \sqrt{\frac{\sum_{k=1}^n (y_k - \hat{y}_k)^2}{n}} \tag{16}$$

Where, n is the number of training data samples, y_k is the actual value, and \hat{y}_k is the predicted value. Through 200 interactions, the fitness curves of stress’s FV-SVR (FV-SVR1), strain’s FV-SVR (FV-SVR2), and low-cycle fatigue life’s FV-SVR (FV-SVR3) of the blade are shown in Figure 5. The RMSE of the FV-SVR model in the three failure modes is 7.2413e-05, 6.1959e-05 and 0.012922. The optimal parameters (c, v, σ, λ, d) searched by the GA are assigned to the FV-SVR model. Through training, the FIMERSM model coefficients for stress, strain and life are shown in Eq. (17)-Eq. (19).

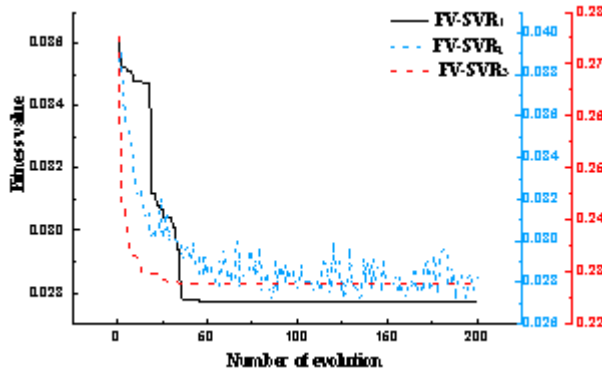


Figure 6 The fitness variation curve of GA

$$\text{Stress} \begin{cases} (a_{ki} - a_{ki}^*)^{(1)} = \begin{bmatrix} -6.5636 & -5.6634 & -0.3530 \\ -5.8734 & 6.5636 & 0.5926 \\ -0.9199 & 1.9129 & -3.8715 \end{bmatrix} \\ c_1, v_1, \sigma_1, \lambda_1, d_1 = [6.560, 0.9495, 0.36602, 0.65748, 1.83] \\ b^{(1)} = 0.2550 \\ \rho(s_x)^{(1)} = 0.4549 \end{cases} \tag{17}$$

$$\text{Strain} \begin{cases} (a_{ki} - a_{ki}^*)^{(2)} = \begin{bmatrix} 1.6893 & 2.5750 & -6.1257 \\ -2.2287 & -4.9128 & -9.7375 \\ -1.1967 & 2.7166 & -1.0232 \end{bmatrix} \\ c_2, v_2, \sigma_2, \lambda_2, d_2 = [3.318, 0.46157, 38.9227, 0.59475, 1.75] \\ b^{(2)} = 0.2604 \\ \rho(s_x)^{(2)} = 0.16395 \end{cases} \tag{18}$$

$$\text{Life} \begin{cases} (a_{ki} - a_{ki}^*)^{(3)} = \begin{bmatrix} -7.7989 & -8.6328 & 8.6328 \\ -2.5999 & 9.1610 & -8.6328 \\ -2.172 & -5.6033 & -4.8285 \end{bmatrix} \\ c_3, v_3, \sigma_3, \lambda_3, d_3 = [8.6328, 0.85414, 1.8475, 0.62242, 1.09] \\ b^{(3)} = -0.0140 \\ \rho(s_x)^{(3)} = 0.18738 \end{cases} \tag{19}$$

2.3. Dynamic Reliability Analysis

In line with the blade working condition and the material parameter [16], the allowable membership function of the stress, strain and life of blade is established, as shown in Figure 6, and the corresponding membership function is expressed as Eq. (20).

$$\begin{aligned}
 u_{G_i}(\sigma) &= \begin{cases} \frac{(x - 578.34)}{30} & \sigma \leq 608.84 \\ \frac{(638.84 - x)}{30} & \sigma > 608.84 \end{cases} & u_{G_i}(\varepsilon) &= \begin{cases} \frac{(x - 0.0000398)}{0.003} & \varepsilon \leq 0.0030398 \\ \frac{(2.0030398 - x)}{2} & \varepsilon > 0.0030398 \end{cases} \\
 u_{G_i}(Nf) &= \begin{cases} \frac{(x - 6914)}{2000} & Nf \leq 8914 \\ \frac{(10914 - x)}{2000} & Nf > 8914 \end{cases}
 \end{aligned} \tag{20}$$

The Eq. (20) is transformed into the form of a probability density function according to the form of Eq. (9). In the case of randomness and fuzziness with input variables, the generalized fuzzy stochastic reliability probabilistic model of the blade is as follows:

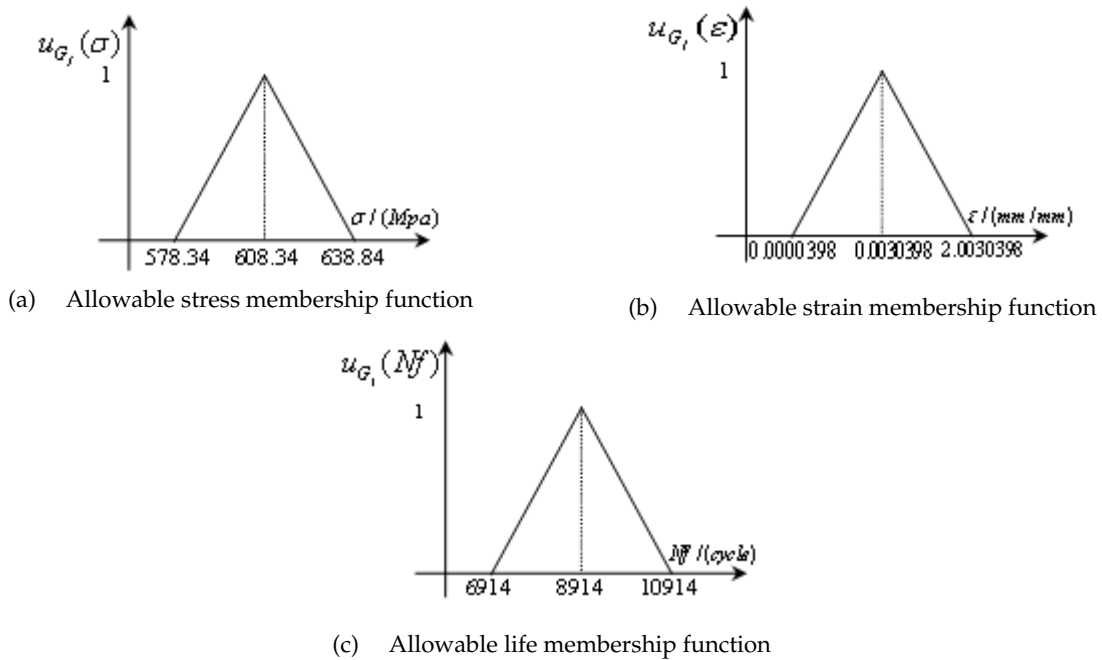


Figure 7 The membership function of the blade allowed constraint

$$\left\{ \begin{aligned}
 p_{r_1} &= \frac{\int u_{G_j}(\sigma) d\sigma}{F} \int_{\Omega_s} \dots \int u_{G_j}^{(e)}(\sigma) \cdot f(\rho) f(w) f(E) f(T_a) f(T_b) f(\sigma' f) f(b) f(\varepsilon' f) f(c) f(W) f(t) f(\delta) f(h) \\
 &\quad d\rho dw dE dT_a dT_b d\sigma' f d\varepsilon' f db dcd W dt d\delta dh \\
 p_{r_2} &= \frac{\int u_{G_j}(\varepsilon) d\varepsilon}{F} \int_{\Omega_s} \dots \int u_{G_j}^{(e)}(\varepsilon) \cdot f(\rho) f(w) f(E) f(T_a) f(T_b) f(\sigma' f) f(b) f(\varepsilon' f) f(c) f(W) f(t) f(\delta) f(h) \\
 &\quad d\rho dw dE dT_a dT_b d\sigma' f d\varepsilon' f db dcd W dt d\delta dh \\
 p_{r_3} &= \frac{\int u_{G_j}(Nf) dNf}{F} \int_{\Omega_s} \dots \int u_{G_j}^{(e)}(Nf) \cdot f(\rho) f(w) f(E) f(T_a) f(T_b) f(\sigma' f) f(b) f(\varepsilon' f) f(c) f(W) f(t) f(\delta) f(h) \\
 &\quad d\rho dw dE dT_a dT_b d\sigma' f d\varepsilon' f db dcd W dt d\delta dh \\
 F &= \int \dots \int u_{G_j}(\sigma) u_{G_j}(\varepsilon) u_{G_j}(Nf) f(\rho) f(w) f(E) f(T_a) f(T_b) f(\sigma' f) f(b) f(\varepsilon' f) f(c) f(W) f(t) f(\delta) f(h) \\
 &\quad d\rho dw dE dT_a dT_b d\sigma' f d\varepsilon' f db dcd W dt d\delta dh
 \end{aligned} \right. \tag{21}$$

By using MCM linkage sampling for FIMERSM model 10,000 times and solve the Eq. (21). The distribution of the output response of the maximum stress point, the maximum strain point and the minimum life point of the blade are shown in Figure 7. The blade reliability analysis results are shown in Table 2.

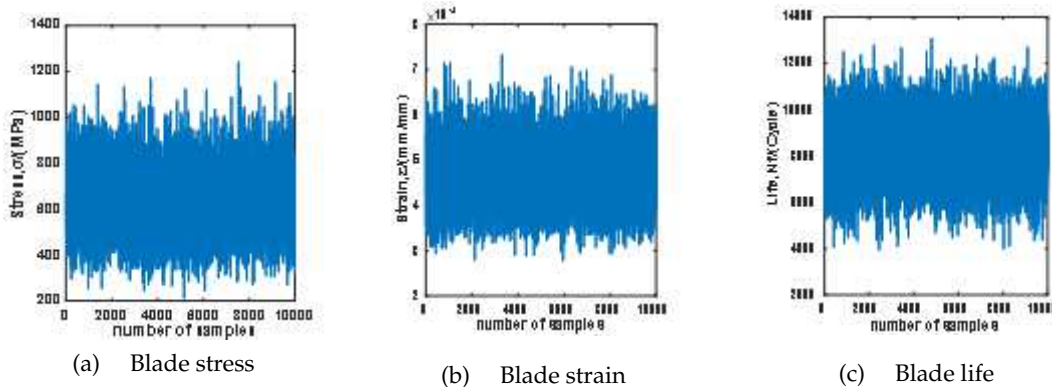


Figure 8 Simulation samples of blade stress, strain and life

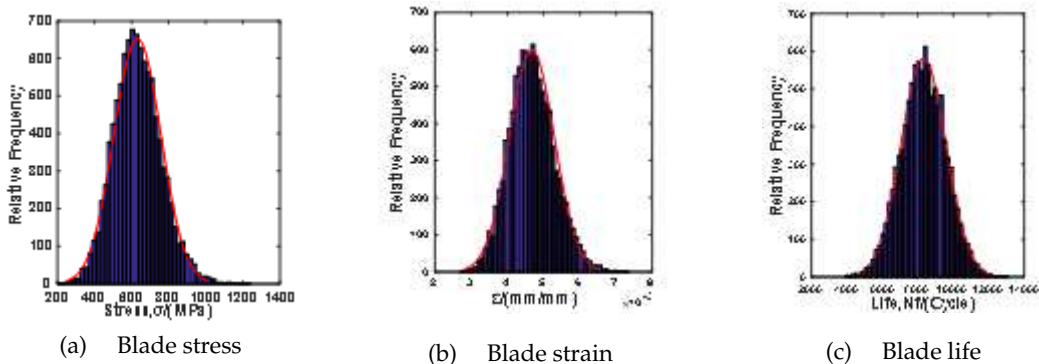


Figure 9 Distribution of blade output response

Table 2 Reliability analysis results of blade

Parameter	Mean	Standard deviation	Failure number	Reliability, (%)	Computational time, (s)
Pr_1 , Stress/MPa	630.076	11.225	40	99.60	0.344
Pr_2 , Strain/mm/mm	0.004674	0.00062114	25	99.75	0.335
Pr_3 , Life/cycle	8312.0022	35.56	29	99.71	0.316
$Pr_1 \cap Pr_2 \cap Pr_3$, Total failure mode	—	—	54	99.46	0.815

3. Validating FIMERSM

To verify the validity of the FIMERSM, the reliability analysis of blade were carried out with MCM, MERSM and FIMERSM according to the input random variables in Table 1 and the same computing environment. Three method computational times are shown in Table 3 and reliability analysis results of blade are listed in Table 4.

Table 3 Computational time of three methods for blade reliability analysis

Method	Different simulations, times				
	10^2	10^3	10^4	10^5	10^6
MCM, ($Pr_1 \cap Pr_2 \cap Pr_3$)	25200 s	14400 s	1209600 s	—	—
MERSM, ($Pr_1 \cap Pr_2 \cap Pr_3$)	0.123 s	3.95 s	6.824 s	16.26 s	—
FIMERSM, ($Pr_1 \cap Pr_2 \cap Pr_3$)	0.094 s	0.359 s	0.815 s	1.537 s	3.162 s

Table 4 Results of blade reliability analysis based on three methods

Sampling number	Reliability degree, ($Pr_1 \cap Pr_2 \cap Pr_3$)			Precision, (%)		Improved precision, (%)
	MCM	MERSM	FIMERSM	MERSM	FIMERSM	
10^2	0.99	0.97	0.99	97	100	3
10^3	0.997	0.988	0.992	99.0	99.4	0.4
10^4	0.9957	0.9913	0.9946	99.55	99.89	0.34
10^5	—	0.99359	0.99832	—	—	—
10^6	—	—	0.999824	—	—	—

4. Discussion

As shown in Table 3, the computational time of FIMERSM is far less than MCM and MERSM. The FIMERSM only spends 0.359 under the 10000 times simulations, which is only 1/8 that of MERSM and 1/1484171 that of MCM.

As shown in Table 4, the computational precision of FIMERSM is higher than MERSM and is almost consistent with MCM. Especially, the computational accuracy of FIMERSM is improved by 0.34% to that of MERSM under 10^4 time simulations.

Additionally, as shown in Table 3 and Table 4, the FIMERSM can solve the reliability analysis problem of multi-failure modes which the MERSM and MCM almost unlikely completed when the simulation times are more than 10^6 .

By the above conclusions, it is fully supported that the FIMERSM not only keeping the high computational precision, but also greatly improve the calculation efficiency.

5. Conclusions and future work

This study proposes a reliability analysis method FIMERSM by integrating FV-SVR and MERSM. The following conclusions are drawn from the simulation:

- 1) The reliability degree of blade stress, strain and fatigue life are 99.60%, 99.75% and 99.71%, respectively.
- 2) FIMERSM is a fast, efficient and accurate method for the reliability analysis of multi-failure mode structure on the premise of guarantee calculation precision.
- 3) In the future, we will focus on the additional factors (creep, crack, etc.) for blade dynamic reliability analysis, and strive to the calculation simulate factors and the actual work of the situation fully consistent.

References

- [1] Bin Bai, Guang-chen Bai. Dynamic probabilistic analysis of stress and deformation for bladed disk assemblies of aeroengine. *Journal of Central South University*, 2014, **21**(10): 3722–3735.
- [2] Mahapatra B S, Mahapatra G S, Roy P K. Fuzzy variable based fuzzy non-linear programming approach for optimization of complex system reliability. *Journal of Intelligent & Fuzzy Systems*, 2015, **28**(4): 1899–1908.
- [3] Mhalla A, Dutilleul S C, Craye E, et al. Estimation of failure probability of milk manufacturing unit by fuzzy fault tree analysis. *Journal of Intelligent & Fuzzy Systems*, 2013, **26**(2): 741–750.
- [4] Pedroso D M. FORM reliability analysis using a parallel evolutionary algorithm. *Structural Safety*, 2017, **65**: 84–99.
- [5] Hu Yun, Liu Shao- Jun, Ding Sheng, et al. Application of response surface method for contact fatigue reliability analysis of spur gear with consideration of EHL. *Journal of Central South University*, 2015, **22**(7): 2549–2556.
- [6] Zhang C Y, Bai G C. Extremum response surface method of reliability analysis on two-link flexible robot manipulator. *Journal of Central South University*, 2012, **19**(1): 101–107.
- [7] Gao H, Fei C, Bai G, et al. Reliability-based low-cycle fatigue damage analysis for turbine blade with thermo-structural interaction. *Aerospace Science & Technology*, 2016, **49**: 289–300.
- [8] Vapnik V N. An overview of statistical learning theory. *IEEE Transactions on Neural Networks*, 1999, **10**(10): 988–999.
- [9] Gururajapathy S S, Mokhlis H, Illias H A B, et al. Support vector classification and regression for fault location in distribution system using voltage sag profile. *Ieej Transactions on Electrical & Electronic Engineering*, 2017.
- [10] Wang X, Wu J, Liu C, et al. A Hybrid Model Based on Singular Spectrum Analysis and Support Vector Machines Regression for Failure Time Series Prediction. *Quality & Reliability Engineering International*, 2016, **32**(8): 2717–2738.
- [11] Sheikhalishahi M. An integrated support vector regression–imperialist competitive algorithm for reliability estimation of a shearing machine. *International Journal of Computer Integrated Manufacturing*, 2016, **29**(1): 16–24.
- [12] Schölkopf B, Smola A J, Williamson R C, et al. New Support Vector Algorithms. *Neural Computation*, 2000, **12**(5): 1207–1245.
- [13] Yan H S, Xu D. An approach to estimating product design time based on fuzzy v-support vector machine. *IEEE Transactions on Neural Networks*, 2007, **18**(3): 721–731.
- [14] Huanrui H. New Mixed Kernel Functions of SVM Used in Pattern Recognition. *Cybernetics & Information Technologies*, 2016, **16**(5): 5–14.
- [15] Zhen-Zhou L U, Sun J. General Response Surface Reliability Analysis for Fuzzy-Random Uncertainty both in Basic Variables and in State Variables. *Chinese Journal of Aeronautics*, 2005, **18**(2): 116–121.
- [16] China Metal Society High Temperature Materials Branch. China Superalloy Handbook. Beijing: China Quality Inspection Press China Standard Press, 2012.p.619-642. (in Chinese)
- [17] Devloo P R B, Rylo E C. Systematic and generic construction of shape functions for p-adaptive meshes of multidimensional finite elements. *Computer Methods in Applied Mechanics & Engineering*, 2009, **198**(21–26): 1716–1725.
- [18] Hashiguchi K. Basic Formulations for Elastoplastic Constitutive Equations. *Elastoplasticity Theory*, 2014, **42**: 135–170.
- [19] Zhang C Y, L C, Fei C W, et al. Multiobject Reliability Analysis of Turbine Blisk with Multidiscipline under Multiphysical Field Interaction. *Advances in Materials Science & Engineering*, 2015, **2015**(5): 519–520.
- [20] Christensen R M. An Evaluation of Linear Cumulative Damage (Miner’s Law) Using Kinetic Crack Growth Theory. *Mechanics of Time-Dependent Materials*, 2002, **6**(4): 363–377.
- [21] Helton J C, Davis F J. Latin hypercube sampling and the propagation of uncertainty in analyses of complex systems. *Reliability Engineering & System Safety*, 2003, **81**(1): 23–69.
- [22] Zhao W, Tao T, Zio E. System reliability prediction by support vector regression with analytic selection and genetic algorithm parameters selection. *Applied Soft Computing*, 2015, **30**(4): 792–802.